Eur. Phys. J. E (2013) **36**: 7
DOI 10.1140/epje/i2013-13007-2

THE EUROPEAN PHYSICAL JOURNAL E

Regular Article

Relaxation of non-equilibrium entanglement networks in thin polymer films

Joshua D. McGraw[1], Paul D. Fowler[1], Melissa L. Ferrari[1], and Kari Dalnoki-Veress[1,a]

Department of Physics & Astronomy and the Brockhouse Institute for Materials Research, McMaster University, Hamilton, Canada

Received 11 October 2012 and Received in final form 7 January 2013
Published online: 29 January 2013 –

Abstract. It is known that polymer films, prepared by spin coating, inherit non-equilibrium configurations which can affect macroscopic film properties. Here we present the results of crazing experiments that support this claim; our measurements indicate that the as-cast chain configurations are strongly stretched as compared to equilibrium Gaussian configurations. The results of our experiments also demonstrate that the entanglement network equilibrates on a time scale comparable to one reptation time. Having established that films can be prepared with an equilibrium entanglement network, we proceed by confining polymers to films in which the thickness is comparable to the molecular size. By stacking two such films, a bilayer is created with a buried entropic interface. Such an interface has no enthalpic cost, only an entropic penalty associated with the restricted configurations of molecules that cannot cross the mid-plane of the bilayer. In the melt, the entropic interface heals as chains from the two layers mix and entangle with one another; crazing measurements allow us to probe the dynamics of two films becoming one. Healing of the entropic interface is found to take less than one bulk reptation time.

1 Introduction

The dynamics of a sufficiently long polymer chain in a melt of like chains will be restricted by topological constraints called entanglements. To a good approximation, each chain in the melt has the configuration of a random walk. Such chains have an "end-to-end" distance —the distance between the ends of the molecule— that scales as the square root of the number of monomers that make up the chain: $R_{\mathrm{ee}} \propto N^{1/2}$. While random walks are not space filling, polymer melts are [1, 2]. The result of this dichotomy is that each melt chain shares its pervaded volume and interacts with many other chains. A fraction of these interactions are entanglements. Though the precise nature of what constitutes an "entanglement" is still unknown, the chains suffer a restricted mobility as a result of these interactions. The collective effect of the entanglements is to create a "tube" in which the molecule is confined [1, 2]. The chain's motion, termed "reptation", is restricted predominantly to directions along the tube. It is well known that these entanglement constraints are largely responsible for many phenomena in polymer physics, such as: high melt viscosity [2, 3] and viscoelasticity [4–6]; enhanced adhesion [7, 8]; glassy failure mechanisms [9–11]; pronounced confinement effects [12, 13]; and alterated hydrodynamic boundary conditions [14, 15].

Since the entanglement network of a polymer melt greatly influences many properties, it is important to make the distinction between equilibrium and non-equilibrium melts. If the chain statistics in a melt are not at equilibrium, then the entanglement network will also be out of equilibrium. As such, measurements of the properties listed above are typically affected. There has been significant interest in non-equilibrium network effects: several studies have investigated the effects of preparation and annealing treatments on the viscosity [16, 17], capillary wave spectra [18], thermal expansion [19] and residual stress [20–26] in polymer films. In these studies, the non-equilibrium structure is inherited from the film casting process. During the preparation of films by casting from solution, polymer chains vitrify at non-zero solvent content. The presence of solvent results in chains that are swollen in comparison to melt conformations. Since the solvent is volatile, most of it leaves the system and the chains are forced into configurations that are not typical of the equilibrium melt. Since the lateral extent of a film does not change during this evaporation process, the structure must compress in the direction normal to the film as solvent leaves —annealing above the glass transition temperature, T_{g}, allows these perturbed networks a chance to evolve towards equilibrium. A schematic of the typical experiment, showing a chain with a "non-equilibrium con-

[a] e-mail: dalnoki@mcmaster.ca

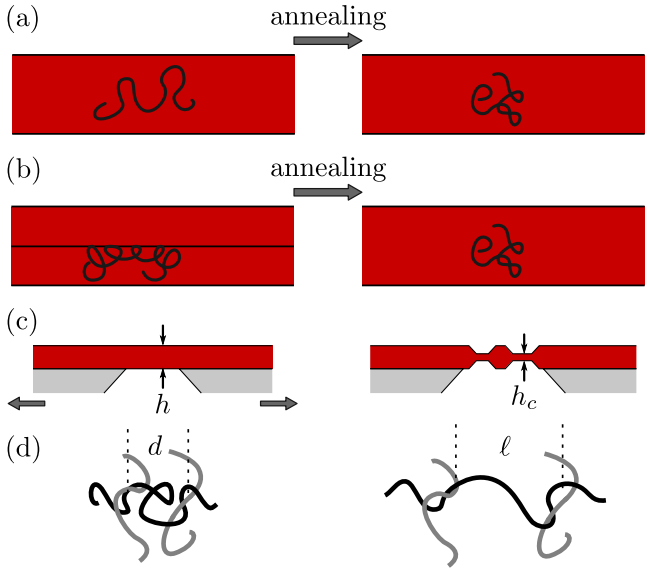

Fig. 1. Schematics of the experiments presented in this work. (a) A chain with a swollen configuration after spin coating. The ensemble of chains recovers equilibrium chain statistics after some period of annealing above T_g. (b) A chain at the "entropic interface" of a bilayer film prepared by stacking two glassy films. Upon annealing above T_g, the Brownian motion of segments allows the entropy-deprived ensemble to relax towards equilibrium. (c) In a crazing experiment, a glassy free standing film with thickness h is strained and necks of material, with thickness h_c are formed. (d) Microscopically, the segments of chains between entanglements have typical size d before straining, and are pulled to a length of ℓ during the crazing experiment.

figuration" being annealed towards an "equilibrium configuration" is seen in fig. 1(a).

The interface of a film also perturbs chain conformations, which results in another method of preparing non-equilibrium samples. Chains at a neutral interface, like a free air or vacuum surface, were described by Silberberg [27]. According to Silberberg's reflection principle, chains that in the absence of a boundary would cross it are instead reflected back into the melt. These chains are thus unable to explore some conformations resulting in a loss of entropy. The significance of this entropy loss has been discussed in relation to the number of inter-chain entanglements, those between two different chains, that exist near an interface [12]. In [12], Brown and Russell suggest that there is a reduction in the number of inter-chain entanglements near an interface; corresponding measurements support this idea [13,15,28]. In these studies, a distinction is made between inter-chain entanglements and those that occur between two segments far apart on the same chain. In light of the chain packing models [29,30] which define entanglements through the interactions of a test chain with other chains, in [13] it was proposed that inter-chain entanglements and intra-chain entanglements do not contribute equally to the integrity of the network. The topological difference between inter- and intra-chain entanglements was suggested to be responsible for the observed thickness dependence of crazing experiments on thin glassy films [13].

While it is possible for polymer chains in a film to be in equilibrium with a reflective boundary, it is also possible to destroy that equilibrium by stacking two such films. This bilayer film results in a sample with what we will refer to as an "entropic interface" —an interface that has an entropic cost associated with the restricted configurations of the molecules that do not cross the mid-plane of the bilayer. As chain segments undergo Brownian motion when annealed above T_g, entropy is recovered as the chains explore a larger pervaded volume. This experiment is schematically depicted in fig. 1(b).

The literature on chains crossing such entropic interfaces is vast. In particular, early experiments by Klein [31] and others [32–34] were some of the first to put on firm footing the reptation arguments [1,2,35] that have been crucial to understanding the physics of long chain polymer melts. In other experiments, the fracture energy is measured as a function of annealing time between the interfaces [36]. Reptation arguments have been employed to understand these results [7,37,38] and simulations are used to investigate these problems [39]. Up to now, however, direct measurements of the entanglement density across an atomically smooth entropic interface have not been made, in part because we have few experimental probes to quantify this property.

As mentioned above, entangled polymeric materials can fail in a way that is distinct from many other modes of glassy failure. The difference arises from the glass being composed of an entangled polymer network. This failure mode, called crazing [9,10,40,41], is like the ductile failure that occurs in metals in that a drawing stress can produce "necks" of deformed material. However, the crazing process is quite different on a molecular level, as the drawn material has a fibrillar structure in which the polymer chains have configurations that are strongly non-Gaussian. The fibrillar material in a craze is characterized by an extension ratio, λ, defined by the ratio of the craze width, to the width of undeformed material that went into forming the craze. If a thin film with thickness h is crazed, using conservation of volume and assuming that the density of the crazed film and unperturbed film are the same, it can be shown that $\lambda \propto h/h_c$, where h_c is the average thickness of crazed material [13,42–44]. A schematic of the crazing process in a thin film is shown in fig. 1(c).

Donald and Kramer [45,46] proposed that for equilibrated polymer films the extension ratio can be understood by assuming that entanglements act like chemical cross links, which remain fixed throughout the crazing process. While a polymer glass is being crazed, the chain segments between entanglements (entanglement strands), with entanglement molecular weight M_e, are extended such that the distance between entanglements after crazing is $\ell \propto M_e$. Polymer chains undergo random walks down to length scales approaching the monomer size, thus the end-to-end distance of the entanglement strand before crazing was $d \propto M_e^{1/2}$. Since the macroscopic response is

a result of the microscopic process, the extension ratio of the craze is the same as that for an average entanglement strand. Therefore, we have $(h_c/h)^2 \propto (d/\ell)^2 \propto 1/M_e$. By recognizing that the density of entanglements is inversely proportional to the mass of a chain segment between entanglements, we have the relation

$$\left(\frac{h_c}{h}\right)^2 \propto \nu_{\text{eff}}, \tag{1}$$

where ν_{eff} is the density of effective entanglements that would be present in a system of equilibrated Gaussian chains. Therefore, by making a measurement of the essentially macroscopic extension ratio, we directly gain information about the microscopic entanglement network. This model was verified by Donald and Kramer [45,46] in experiments, was observed in molecular dynamics simulations by Rottler and Robbins [40,41], and has since been used in many other experiments [10,13,44,47].

In this work, we take advantage of the fact that measuring the craze extension ratio provides information about the entanglement network [13,44] to gain insight into the equilibration process of two non-equilibrium polymer entanglement networks. In the first case, we examine the dependence of the measured $(h_c/h)^2$ on the temperature and subsequent annealing time. After learning how to equilibrate an entanglement network, insomuch as the crazing measurement is concerned, we turn to the creation and healing of the entropic interface provided by a bilayer film.

2 Experiment

Polystyrene (PS) with weight averaged molecular weights $M_w = 785$ and 1144 kg/mol and polydispersity indices ≤ 1.07 (Polymer Source, Inc.) were used to prepare the samples; we refer to these as PS(785k) and PS(1144k). Polymer of a given molecular weight was dissolved into toluene (Fisher Scientific, Optima grade) in various weight fractions ($0.5 < \phi < 2.5$ wt%) and spin coated onto freshly cleaved, $30 \times 30\,\text{mm}^2$ mica sheets (Ted Pella, Inc., Hi-Grade, V2). Spin coating was carried out at room temperature in air; however, in order to explore the effects of temperature several films were also prepared with the substrate attached to a temperature controlled spin coater chuck. The chuck, an aluminum plate in intimate contact with the substrate, ranged in temperature from $5 \leq T \leq 40\,^\circ\text{C}$. Since the thermal mass of the mica substrate and PS/toluene solution is small compared with that of the spin coater chuck, we assume that the solution temperature at the onset of spin coating is close to that measured on the chuck. Because the temperature gradients are large due to the evaporative cooling of the solvent, the temperature controlled measurements serve only to vary the initial temperature of spin coating. For all monolayer experiments of the type depicted in fig. 1(a), samples were 105 ± 10 nm thick and composed of PS(785k). Note that we use the terminology "monolayer" to describe a sample consisting of a single film, rather than a molecular monolayer; we refer to two such films stacked on top of one another as a "bilayer". For the study of spin coating effects, monolayers were annealed at $130 \pm 1\,^\circ\text{C} > T_g \approx 97\,^\circ\text{C}$ in a home built vacuum oven (pressure $\sim 10^{-5}$ mbar provided by a turbo molecular pump), for times $0 \leq t_m \leq 348$ hr. Here and throughout, the subscript "m" refers to monolayer samples.

In order to prepare bilayer films, we first followed the above procedure for monolayer preparation, except that the monolayers were prepared from PS(1144k), were 50 ± 3 nm thick, and annealed at 150 °C for $t_m = 48$ hr[1]. We note that this thickness was chosen such that the monolayers, as described in the work of Si and co-workers [13], would show a thickness dependent $(h_c/h)^2$, while a film with twice the monolayer thickness would be in a range for which $(h_c/h)^2$ had saturated. After annealing, a monolayer was floated onto the surface of an ultra pure water bath (18.2 MΩ cm, Pall, Cascada LS) and a second monolayer, still on a mica substrate, was placed onto the floating monolayer with the polymer-side down, thus creating a PS bilayer[2]. After preparation, the bilayers were annealed for periods $0.5 \leq t_b \leq 90$ hr at 130 °C (subscript "b" refers to bilayers) in vacuum ovens or on a microscope hot stage (Linkam) in air. The temperature is always known to within 1 °C.

With mono- and bilayers prepared, $\sim 9 \times 9\,\text{mm}^2$ sections of the films were floated onto the surface of an ultra clean water bath and were picked up using a set of two polished and sharp aluminum blocks. The blocks had a fixed gap of $l = 1.5$ mm between the two sharp edges. After drying, one of the blocks was held in place while the other was attached to a translation stage (Newport MFA-CC, SMC100CC). The blocks were then unfixed and the film was deformed with a strain rate of $\dot{\Delta l}/l = 2 \times 10^{-4}\,\text{s}^{-1}$ until crazes were visible under an optical microscope, see fig. 1(c). The samples were typically strained to $\Delta l/l = 0.1$, which resulted in a film with both crazed and undeformed material. Typical craze widths were $\sim 10\,\mu$m.

Crazed PS films ($\sim 1.5 \times 9\,\text{mm}^2$) were placed onto $10 \times 10\,\text{mm}^2$ Si wafers. Surface forces pull the crazed film that bridges the aluminum gap into contact with the wafer, thereby transferring the delicate sample to the robust Si surface [13,44]. Scratches were put into the film using a scalpel blade. By measuring an appropriate spot along the edge of a scratch, we are able to simultaneously measure the undeformed film height, h, and the height of the craze, h_c relative to the Si substrate surface. An example of such a measurement is shown in fig. 2.

[1] As will become clear below, this time is sufficient to ensure an equilibrium entanglement network within the resolution of our experiment

[2] One particular advantage of doing these experiments with spin-coated monolayers is that the surfaces have a highly uniform topography (rms roughness ~ 0.3 nm as measured with AFM), ensuring intimate contact between the interfaces. A second advantage of this approach is the fact that we prepare an entropic interface while ensuring that the chains at that interface will not have suffered chain scission. Thus, we can assume a monodisperse chain length distribution at the interface.

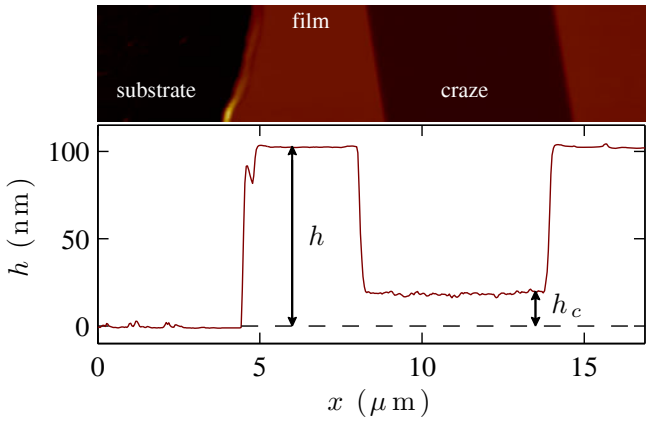

Fig. 2. Height as a function of position from an AFM experiment for a typical crazed thin film after transfer to a Si substrate. From data sets such as these, the film height h, and the craze height h_c are easily determined.

3 Results and discussion

This section is broken into two parts. First, we describe the results of experiments on simple monolayer PS films as shown in fig. 1(a): both the state of as-cast films, and the evolution of these films towards equilibrium will be discussed. We establish that, with extensive annealing above T_g, films may be prepared such that they display the same entanglement density as that of the bulk. Then, we discuss our results on bilayer films with a buried entropic interface, as shown schematically in fig. 1(b).

3.1 Monolayers

3.1.1 As-cast films

In fig. 3(a) is shown a plot of the measured ratio $(h_c/h)^2$ as a function of the temperature of the spin coater chuck on which films were prepared. Additionally, the inset of fig. 3(a) shows the data obtained at $T = 20\,^\circ$C in the main figure. For each trial number, data is grouped according to preparation under a given set of experimental conditions. The data in the inset was obtained at room temperature using various initial solution concentrations, while adjusting the spin speed to ensure constant resultant thickness. Additionally, we varied the toluene solvent content in the atmosphere during spin coating. It is clear from the inset that there is considerable scatter in the resulting $(h_c/h)^2$.

In fig. 3(b) are shown two histograms of $(h_c/h)^2$ for films prepared on a spin coater chuck at $T = 5$ and $30\,^\circ$C; N is the number of measurements of the type shown in the plot of fig. 2. Each data point in figs. 3, 4 and 5 is the mean value of such a distribution: in figs. 3 and 4, the distance from the bottom to the top of an error bar is one standard deviation of the distribution. As such, the reported error in these figures indicates the range of expected values one might obtain from an experimental measurement of $(h_c/h)^2$.

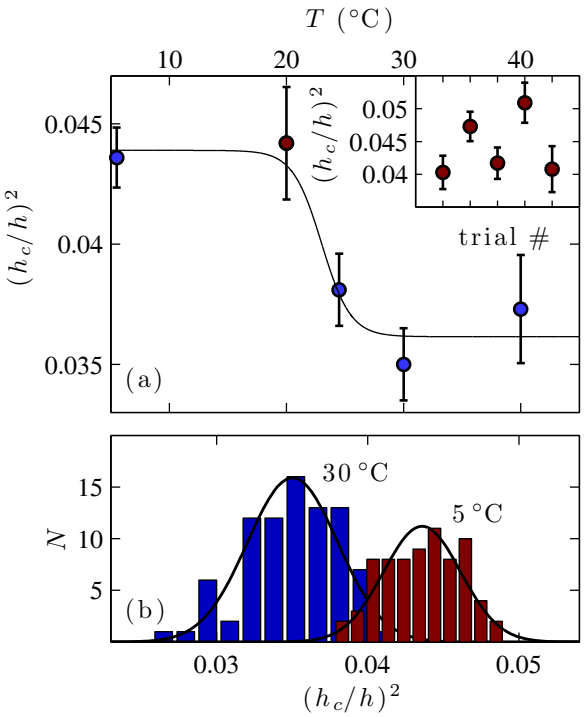

Fig. 3. (a) Plot of $(h_c/h)^2$ for PS(785k) films with thickness 105 ± 10 nm as a function of the temperature of the spin coater chuck on which the films were prepared. The data point in red at $T = 20\,^\circ$C is detailed in the inset. There, data from films prepared at room temperature under different casting conditions are shown (different solution concentrations and atmospheric solvent content). The solid black line is a guide for the eye. (b) Histograms for a number of measurements of the type shown in fig. 2. For all data in (a), error bars represent are standard deviations from distributions of the type shown in (b).

The data of fig. 3 indicate that $(h_c/h)^2$ of as-cast films is sensitive to the temperature of the spin coater chuck on which they are prepared. Furthermore, at a given temperature, this quantity is non-trivially dependent on the preparation conditions; even at room temperature the data spread is 20% of the mean value measured at room temperature. Despite our best efforts, we find that there is great variation in the measured values of $(h_c/h)^2$ for films cast with the same initial chuck temperature.

In fig. 4, we see that the values of $(h_c/h)^2$ at $t_m = 0$ (no annealing above T_g) are enhanced as compared to the data at late times. As explained in detail below, chain stretching can account for an enhanced $(h_c/h)^2$ as compared to the measured equilibrium values at long times in fig. 4. Thus, we will now describe two mechanisms by which chains in the as-cast state may become swollen or stretched as compared to their melt equilibrium. We note that while the experimental results provide a robust characterization of the films, the interpretation of the as-cast data is speculative.

The first mechanism we consider results from the fact that chains in the presence of an athermal solvent are swollen in comparison to the melt. The well-established

crazing model, described in the introduction, tells us that $(h_c/h)^2 \sim \nu_{\rm eff}$ is valid for equilibrated films because it is based on the Gaussian random statistics of polymer chains: $d \propto M_e^{1/2}$. Clearly, we must take care to interpret the measured values of $(h_c/h)^2$ plotted in figs. 3 and 4 as simply proportional to the entanglement density. More generally, the entanglement segments can have end-to-end distance $d \propto M_e^n$, see fig. 1(d). While for equilibrated polymer films, $n = 1/2$, here we assume $n > 1/2$ since the chain configurations are formed during the spin coating process while still swollen by solvent. After crazing, the segments between entanglements are stretched and we have $\ell \propto M_e$. Following the same logic that precedes eq. (1), we have $h_c/h \propto d/\ell \propto M_e^{n-1}$. Thus, if $n > 1/2$ for swollen chains, then for constant M_e, the measured value of $(h_c/h)^2$ will be larger as compared to an equilibrated system. The enhancement would be due to the fact that swollen chains can be stretched less before having to draw new material into a craze[3].

The second mechanism which can explain an enhanced value of $(h_c/h)^2$ for as-cast films is due to the hydrodynamics of spin coating. During spin coating a polymer solution is deposited onto a substrate at rest. From rest, the substrate is rapidly rotated, producing considerable shear at the substrate-solution interface. As described by Emslie and co-workers several decades ago [48], the height profile of the liquid atop the substrate quickly becomes flat and there is a radial flow that is balanced by a viscous Poiseuille flow in the vertical direction. This flow produces shear both in the plane of and in the direction normal to the substrate. The shear may be large enough for polymer chains to become oriented to the flow. At vitrification, these flow oriented chains would become trapped in configurations that are stretched in comparison to Gaussian chains. This stretching would result in an enhanced value of $(h_c/h)^2$.

In the studies by Steiner and co-workers [16, 17], the apparent viscosity of as-cast polymer films is measured using an electro-hydrodynamic method. Their films, prepared on Si from PS and toluene solutions, showed a decrease in the viscosity of the as-cast state as compared to annealed films. Tsui and co-workers [18] also measure the viscosity of PS films on Si cast from solvents of various quality, ranging from $T \lesssim \Theta$, with Θ the temperature at which chain dimensions are indistinguishable from the melt, to $T > \Theta$ (by contrast, our films are always prepared with $T \gg \Theta$). Using a method of spectral analysis, they find the viscosity of as-cast films to be reduced from its value at long annealing times. All of these results are consistent with a reduced entanglement density in as-cast films, and this idea is often invoked to explain these types of observations. If the interpretation of our results for as-cast films is to be consistent with the reduced entanglement density claimed by others, then it must be that the chain configurations trapped in the as-cast films are stretched beyond that of typical Gaussian chains (either due to swelling by solvent or hydrodynamic shearing effects). Since we measure an enhanced $(h_c/h)^2$ in the as-cast state, it must be that the degree of chain stretching we observe is quite severe. A lower entanglement density with Gaussian statistics would lead to a depressed $(h_c/h)^2$; thus, the stretching and swelling must be enough to dominate this effect. Support for this chain stretching idea can be found in the systematic studies of the pre-stress in spin-coated polymer films [20–24]. Specifically, Reiter and co-workers [19,22,23,26] have used dewetting to probe the behaviour of as-cast films. They observe that the radius of a dewetting hole is larger for an as-cast film when compared to a hole grown for an identical period in a film aged below T_g. In these works, the idea of molecular chain stretching is precisely the supposed origin of the studied pre-stress.

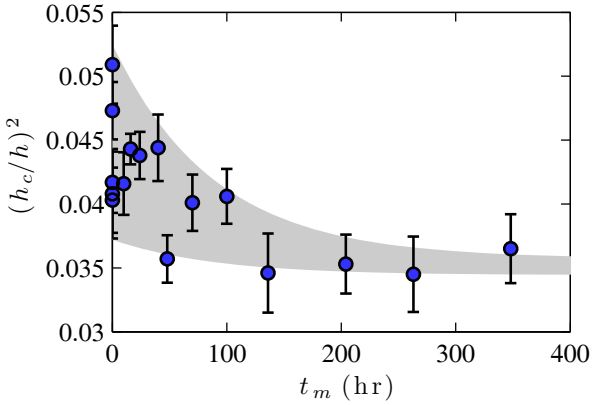

Fig. 4. $(h_c/h)^2$ for PS(785k) monolayers with thickness 105 ± 10 nm spin cast and annealed for times t_m at 130 °C. Since the non-equilibrium state at $t_m = 0$ could not be well controlled, there are a range of values reported. We expect a measurement at subsequent annealing times to be found anywhere within the shaded region.

We now turn to the dependence of $(h_c/h)^2$ on the temperature of the spin coating chuck. The temperature range shown in fig. 3 is high enough so that the PS chain statistics in toluene can be considered as athermal; that is, the average size of an isolated chain in solution does not vary significantly with temperature. Therefore, with this solvent we cannot attribute the observed temperature dependence of $(h_c/h)^2$ to changes in the solvent quality of the film preparation. The solvent quality was claimed as the dominant effect responsible for some of the rheological behaviour seen in previous studies [18, 19, 23]. During the spin coating process, solvent continuously evaporates and the sample vitrifies at a non-zero solvent content. At a lower initial chuck temperature, the sample vitrifies with a higher solvent concentration than at a higher initial temperature. Therefore, without considering the highly violent, non-equilibrium process of spin coating, the chains in films prepared at lower temperatures are necessarily more swollen than their counterparts prepared at higher temperatures. As discussed above, crazing a sample in which the chains were trapped in pre-stretched configurations may account for the general trend of higher $(h_c/h)^2$ observed at lower temperatures in fig. 3.

[3] In [42,43], it is shown that crazes grow in width by continuously drawing new material from the undeformed film and maximally stretching this new material, before drawing in more.

To summarize our results on the as-cast monolayer films, we find that the measured value of $(h_c/h)^2$ is enhanced in an as-cast film as compared to a film annealed above T_g for long times (see fig. 4). We propose that the enhancement is due to pre-stretching of the chains during the spin coating process that may occur because of solvent swelling or hydrodynamic shearing. Lastly, the initial temperature at which spin coating proceeds greatly affects the nature of entanglements in as-cast films, even for films prepared from an athermal solvent.

3.1.2 Temporal evolution of as-cast films towards equilibrium

Given the sensitive temperature and environmental dependence of the as-cast extension ratio, the as-cast chain configurations cannot represent those of the equilibrium melt. As such, high-temperature annealing, with $T > T_g$, is expected to result in an evolution towards the equilibrium melt chain statistics. Following a quench to room temperature after an annealing treatment, we would expect to observe differences in $(h_c/h)^2$. In fig. 4 are shown the results of experiments, using PS(785k), for which films were annealed for various times, t_m, before crazing. The data in the inset of fig. 3(a) is shown at $t_m = 0$. As described above, it can be seen that the as-cast state has a larger $(h_c/h)^2$ than for longer annealing times. The data plateaus on a time scale $\tau_m \approx 80\,\mathrm{hr}$. To extract this time scale, we have performed a best fit to all the data using an exponential function: $(h_c/h)^2 = A_m + B_m e^{-t_m/\tau_m}$. The best fit parameters were $A_m = 0.035$, $B_m = 0.010$ and $\tau_m = 80\,\mathrm{hr}$.

From the data at $t_m = 0$ in fig. 4, we can see that our preparation under standard laboratory conditions yields a spread of measured $(h_c/h)^2$. However, independent of the preparation, thermal annealing brings all samples toward the same equilibrium state. Within the error of our experiment, all values of $(h_c/h)^2$ after $t_m = 100\,\mathrm{hr}$ are the same. The longest relaxation time of a polymer melt is the reptation time, τ_{rep}, which represents the typical time taken for a molecule in the bulk to lose memory of all previous strains [2]. For PS(785k) at 130 °C, the reptation time is approximately 35 hr [49]. Thus we conclude that the out-of-equilibrium network of the as-cast films relaxes on a time scale ($\tau_m = 80\,\mathrm{hr}$) that is on the order of one reptation time ($\tau_{rep} \sim 35\,\mathrm{hr}$).

In the work by Steiner and co-workers [16,17] as well as Tsui and co-workers [18] described above, the viscosity is probed. In these cases, the time constants for the evolution of the viscosity towards equilibrium is found to be between two and five orders of magnitude longer than the bulk reptation time. These measurements are in stark contrast to the crazing results presented here. As a possible explanation for the discrepancy, we note that in the measurements of Steiner and coworkers, the film surface is perturbed by only $\sim 5\,\mathrm{nm}$ —a distance that is similar to the distance between entanglement points, or tube-diameter, of PS [29]. Similarly, in the experiments of Tsui and co-workers, it is the capillary wave spectra that are measured, and variations in the height of the samples in the sub-nanometre regime are typical. In addition, the capillary wave measurements are carried out on 14 nm thick samples, which may already be thin enough to observe confinement effects. Thirdly, Napolitano and Wübbenhorst [50] observe that changes in the dielectric response of thin PS films on aluminum substrates take up to 3 orders of magnitude longer than the bulk reptation time. Their results are attributed to the formation of an adsorbed polymer layer that is between 4 and 8 nm thick. By contrast, in the crazing measurement the entire film of $\sim 100\,\mathrm{nm}$ thickness is probed —crazing reports a "bulk" film property. It is then possible that the origin of the significant discrepancy in relaxation time scales is the result of a subtle and interesting effect which is particular to the interfacial regions of the polymer films studied in [16–18,50].

3.2 Bilayers

In the previous section, we discussed that as-cast films are characterized by a non-equilibrium entanglement network. Furthermore, we established that the as-cast films can be equilibrated on time scales comparable to the longest relaxation time of the polymer. We now turn to the results observed in another non-equilibrium entanglement network: bilayer films with a buried entropic interface, as shown schematically in fig. 1(b).

As discussed in the introduction, chains at an interface are subject to the Silberberg reflection principle [1,12,27], which states that chain segments that would have crossed the interface are instead reflected back into the polymer melt. These chains thus share their pervaded volumes with fewer other chains, compared to chains in the bulk (see p. 61 in [1]). The influence of the reflection principle on the measurement of $(h_c/h)^2$ was exploited by Si and co-workers [13]. It was found that a film whose thickness is similar to the unperturbed coil radius has a lower $(h_c/h)^2$. The results were interpreted as being due to a reduced inter-chain entanglement density at an interface, similar to ideas first proposed by Brown and Russell [12].

In our experiments, the monolayers used to prepare the bilayers were thin enough to have $(h_c/h)^2$ values that are markedly different from the thick film regime as measured by Si and co-workers [13]; while the end-to-end distance of PS(1144k) is approximately 70 nm [51], the bilayers were made from two films with $h \approx 50\,\mathrm{nm}$. These monolayers were annealed as described in the experimental section, with annealing times $t_m > 10\,\tau_{rep}$ [49]. Given the results of fig. 4, we assume that the resulting monolayers had chain statistics described by the equilibrium value corresponding to the confined films. We stress that the thickness of the monolayers was chosen specifically: the monolayers are thin enough such that they exhibit a reduced effective entanglement density, while a film thickness corresponding to twice that thickness has a bulk-like entanglement density according to the work by Si and co-workers [13]. Thus, a bilayer film will show a reduced $(h_c/h)^2$ which approaches the bulk value upon annealing.

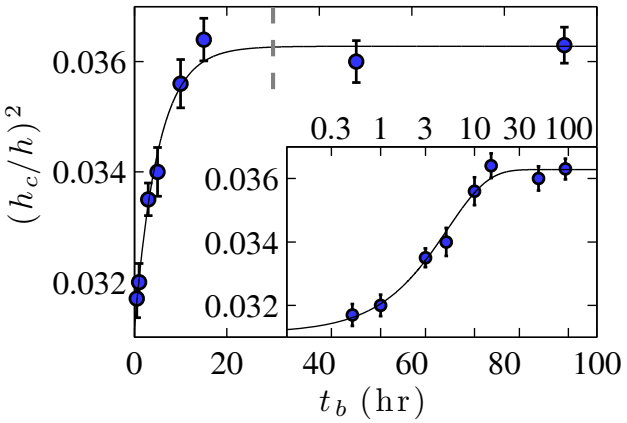

Fig. 5. $(h_c/h)^2$ as a function of annealing time, t_b at 130 °C, for PS(1144k) bilayer samples prepared by stacking two monolayer films with thickness 50±3 nm. The error bars in this figure are the standard error of the mean, rather than the standard deviation as reported in figs. 3(a) and 4. The vertical dashed line indicates $\tau_{rep}/4$. To emphasize the data at early times and the agreement with an exponential relaxation, the inset shows the same data as in the main figure, except with a logarithmic time axis.

In fig. 5 are shown the results of measurements on bilayer films annealed for times t_b at $T = 130\,°C$, well above T_g. The errors reported are the standard error of the mean as taken from distributions similar to those in fig. 3(b). The data in fig. 5 is well described by an exponential: $(h_c/h)^2 = A_b - B_b e^{-t_b/\tau_b}$. The best fit to the data corresponds to $A_b = 0.0363$, $B_b = 0.0051$ and $\tau_b = 5.1$ hr. Given that the reptation time of PS(1144k) at 130 °C is approximately equal to 120 hr, we find that the relaxation across the entropic interface is achieved much faster than one bulk reptation time. Since at $t_b = 0$ there are no entanglements across the interface, and after equilibration the bulk-like entanglement density is achieved, we can interpret the increase in $(h_c/h)^2$ as a direct measure of the change in entanglement density across the interface.

Here we consider the scenario in which a molecule is most severely confined by the entropic interface. This occurs when the molecule's centre of mass would have been found at the location of the interface in the absence of a barrier (see fig. 1(b)). In this case, the chain's average pervaded volume is exactly half of that in the bulk. Since a molecule in this state is maximally perturbed, this scenario provides an upper bound on the time it takes the bilayers to lose memory of the entropic interface. Even though polymer chains are confined near a reflecting boundary, we expect the molecules to move predominantly by reptation. This is the assumption that has been made in models used to explain, for example, the recovery of fracture toughness of polymer-polymer interfaces, and more generally the diffusive processes across these interfaces [7, 36, 37]. A molecule that is maximally perturbed must relax such that its pervaded volume increases by a factor of two. By analogy with molecular relaxation in the bulk, the molecule must diffuse by a distance of roughly $R_{ee}/2$ to lose the memory of its confinement. Notwithstanding the possibility that the dynamics of polymer chains at an interface may be altered by confinement [28], the diffusion equation dictates that the time it takes for a typical bulk polymer chain to diffuse by a distance $R_{ee}/2$ corresponds to a time $\tau_{rep}/4$. Thus, by making a simple bulk reptation argument, and invoking the reflection principle, we find that the maximum time taken to lose memory of the bilayer interface is less than τ_{rep}. In fig. 5, we have inserted a vertical dashed line at $t_b = \tau_{rep}/4$. The data has clearly saturated by this time. The relaxation time that we measure, τ_b, is representative of the average relaxation time for perturbed chains near the interface, with $\tau_{rep}/4$ being an upper bound.

3.3 Equilibria of as-cast monolayer and bilayer films

A condition for equilibrium is that a system can arrive at the state independent of the initial condition. In the previous two sections of this work, we have described the preparation and evolution towards equilibrium of two non-equilibrium states: as-cast monolayer films and bilayers prepared with an entropic interface. In both cases, we observe that after a sufficient relaxation time $(h_c/h)^2$ reaches a plateau. Examining the long time behaviour of figs. 4 and 5 we see that, within error, both non-equilibrium systems reach the same plateau value having started from different initial conditions. That $(h_c/h)^2$ is independent of the preparation after long annealing times is a strong indication that these films are at true equilibrium. To qualify this statement, we cannot rule out long term changes beyond the resolution of the crazing measurement.

4 Conclusion

We have performed a series of crazing measurements designed to probe non-equilibrium states of thin polymer films. In the first case, we examine the effect of spin coating on the resulting craze characteristic, $(h_c/h)^2$. We find that the as-cast films display strongly non-equilibrium behaviour that is difficult to control even under seemingly identical initial conditions. The measured values of $(h_c/h)^2$ can be reconciled with results from other researchers [16–19, 22, 23, 26] if we interpret the as-cast films as having trapped molecular configurations that are stretched compared to the equilibrium Gaussian statistics. Thermal annealing of these films results in an approach to a plateau in $(h_c/h)^2$, and the equilibration time is consistent with relaxation on a time scale comparable to the polymer reptation time.

Having established that it is possible to prepare monolayer films with an equilibrium entanglement density, we measured $(h_c/h)^2$ in bilayers prepared by stacking two monolayer films. Such a bilayer film is then chemically equivalent to a film with the thickness of two monolayers, but differs in that there is an entropic interface. The interface has no enthalpic penalty and only a diminished entropy due to fewer available molecular configurations.

The monolayers were chosen such that they confine the long chain molecules resulting in a reduced effective entanglement density, while a film of twice the monolayer thickness exhibits a bulk-like entanglement density. We find that the as-prepared bilayers craze in a way that is consistent with previously reported measurements on confined monolayers. Thermal annealing above T_g causes the entropic interface in the middle of the bilayer to heal, effectively converting the bilayer into a single film. The healing of the entropic interface occurs on a time scale that is shorter than one bulk reptation time.

Financial support from NSERC of Canada is gratefully acknowledged.

References

1. P.G. de Gennes, *Scaling Concepts in Polymer Physics* (Cornell University Press, 1979).
2. M. Rubinstein, R.H. Colby, *Polymer Physics* (Oxford University Press, 2003).
3. G.C. Berry, T.G. Fox, Adv. Polym. Sci. **5**, 261 (1968).
4. J.D. Ferry, *Viscoelastic Properties of Polymers*, 3rd edition (John Wiley & Sons, Inc., 1980).
5. T.C.B. McLeish, Adv. Phys. **51**, 1379 (2002).
6. A.E. Likhtman, T.C.B. McLeish, Macromolecules **35**, 6332 (2002).
7. H.H. Kausch, M. Tirrell, Annu. Rev. Mater. Sci. **19**, 341 (1989).
8. C. Creton, E.J. Kramer, H.R. Brown, C.-Y. Hui, Adv. Polym. Sci. **156**, 53 (2001).
9. E.J. Kramer, Adv. Polym. Sci. **52/53**, 1 (1983).
10. E.J. Kramer, L.L. Berger, Adv. Polym. Sci. **91/92**, 1 (1990).
11. H.R. Brown, Macromolecules **24**, 2752 (1991).
12. H.R. Brown, T.P. Russell, Macromolecules **29**, 798 (1996).
13. L. Si, M.V. Massa, K. Dalnoki-Veress, H.R. Brown, R.A.L. Jones, Phys. Rev. Lett. **94**, 127801 (2005).
14. F. Brochard-Wyart, P.G. de Gennes, H. Hervet, C. Redon, Langmuir **10**, 1566 (1994).
15. O. Bäumchen, R. Fetzer, K. Jacobs, Phys. Rev. Lett. **103**, 247801 (2009).
16. D.R. Barbero, U. Steiner, Phys. Rev. Lett. **102**, 248303, (2009).
17. K.R. Thomas, A. Chenneviere, G. Reiter, U. Steiner, Phys. Rev. E **83**, 021804 (2011).
18. R.N. Li, A. Clough, Z. Yang, O.K.C. Tsui, Macromolecules **45**, 1085 (2012).
19. A. Clough, M. Chowdhury, K. Jahanshahi, G. Reiter, O.K.C. Tsui, Macromolecules **45**, 6196 (2012).
20. S.G. Croll, J. Appl. Polym. Sci. **23**, 847 (1979).
21. G. Reiter, M. Hamieh, P. Damman, S. Sclavons, S. Gabriele, T. Vilmin, E. Raphaël, Nat. Mater. **4**, 754 (2005).
22. P. Damman, S. Gabriele, S. Coppée, S. Desprez, D. Villers, T. Vilmin, E. Raphaël, M. Hamieh, S. Al Akhrass, G. Reiter, Phys. Rev. Lett. **99**, 036101 (2007).
23. A. Raegen, M. Chowdhury, C. Calers, A. Schmatulla, U. Steiner, G. Reiter, Phys. Rev. Lett. **105**, 227801 (2010).
24. K.R. Thomas, U. Steiner, Soft Matter **15**, 7839 (2011).
25. F. Closa, F. Zeibert, E. Raphaël, Phys. Rev. E **83**, 051603 (2011).
26. M. Chowdhury, P. Freyberg, F. Zeibert, A.C.-M. Yang, U. Steiner, G. Reiter, Phys. Rev. Lett. **109**, 136102 (2012).
27. A. Silberberg, J. Colloid Interface Sci. **90**, 86 (1982).
28. H. Bodiguel, C. Fretigny, Phys. Rev. Lett. **97**, 266105 (2006).
29. L.J. Fetters, D.J. Lohse, D. Richter, T.A. Witten, A. Zirkel, Macromolecules **27**, 4639 (1994).
30. L.J. Fetters, D.J. Lohse, W.W. Graessley, J. Polym. Sci. Polym. Phys. **37**, 1023 (1999).
31. J. Klein, Nature **12**, 144 (1978).
32. P.F. Green, E.J. Kramer, Macromolecules **19**, 1108 (1986).
33. Y. Liu, G. Reiter, K. Kunz, M. Stamm, Macromolecules **26**, 2134 (1993).
34. A. Karim, G.P. Felcher, T.P. Russell, Macromolecules **27**, 6973 (1994).
35. P.G. de Gennes, J. Chem. Phys. **35**, 572 (1971).
36. K. Jud, H.H. Kausch, J.G. Williams, J. Mater. Sci. **16**, 204 (1981).
37. S. Prager, M. Tirrell, J. Chem. Phys. **75**, 5194 (1981).
38. F. Brochard-Wyart. *Fundamentals of Adhesion*, Chapter 6 (Plenum Press, New York, 1991).
39. F. Pierce, D. Perahia, G.S. Grest, EPL **95**, 46001 (2011).
40. J. Rottler, M.O. Robbins, Phys. Rev. E. **68**, 011801 (2003).
41. J. Rottler, J. Phys.: Condens. Matter **21**, 463101 (2009).
42. H.R. Brown, J. Mater. Sci. **14**, 237 (1979).
43. B.D. Lauterwasser, E.J. Kramer, Philos. Mag. A **39**, 469 (1979).
44. J.D. McGraw, K. Dalnoki-Veress, Phys. Rev. E **82**, 021802 (2010).
45. A.M. Donald, E.J. Kramer, J. Polym. Sci. Part B: Polym. Phys. **20**, 899 (1982).
46. A.M. Donald, E.J. Kramer, Polymer **23**, 461 (1982).
47. A.C.-M. Yang, E.J. Kramer, C.C. Kuo, S.L. Phoenix, Macromolecules **19**, 2020 (1986).
48. A.G. Emslie, F.T. Bonner, L.G. Peck, J. Appl. Phys. **20**, 858 (1958).
49. A. Bach, K. Almdal, H.K. Rasmussen, O. Hassager, Macromolecules **36**, 5174 (2003).
50. S. Napolitano, M. Wübbenhorst, Nat. Commun. **2**, 260 (2011).
51. J.P. Cotton, D. Decker, H. Benoit, B. Farnoux, J. Higgins, G. Jannink, R. Ober, C. Picot, J. des Cloizeaux, Macromolecules **7**, 863 (1974).